Automatica 50 (2014) 747–755

Contents lists available at ScienceDirect

Automatica

journal homepage: www.elsevier.com/locate/automatica

A regime-switching model with the volatility smile for two-asset European options☆

Junseok Kim [a,1], Darae Jeong [a], Dong-Hoon Shin [b,2]

[a] Department of Mathematics, Korea University, Seoul 136-713, Republic of Korea

[b] Department of Global finance and banking, Inha University, Incheon 402-751, Republic of Korea

ARTICLE INFO

Article history:
Received 15 November 2011
Received in revised form
15 November 2013
Accepted 27 November 2013
Available online 1 February 2014

Keywords:
Regime-switching model
Finite difference method
Operator splitting method
Volatility smile

ABSTRACT

In this paper, we consider a numerical European-style option pricing method under two regime-switching underlying assets depending on the market regime. For a risk neutral market condition, we consider regime-switching model with two assets using a Feynman–Kac type formula. And to solve the option problem with regime-switching model, we apply an operator splitting method. Numerical examples show the volatility smile and the volatility term structure under varying parameters on a two state regime switching model.

1. Introduction

The Black–Scholes (BS) formula for option pricing is widely applied to the pricing of numerous European options; see Haug (1997). The underlying securities of the Black–Scholes formula are supposed to be geometric Brownian motions that contain pairs of two parameters, the expected rate of return and the volatility. Both parameters are assumed to be constants in the general Black–Scholes model, and these assumptions are not applicable to option pricing in real markets. To overcome the shortfall of the BS model, the volatility smile and term structure are used to capture the change in volatility in terms of the price and the maturity of a security.

The regime-switching model is an alternative model to illustrate the stochastic volatility. Since stock parameters practically are depended on the market mode that switches among a finite number of states, we naturally allow the key parameters of the underlying assets to reflect a random market environment.

The regime-switching model is invoked to formulate such parameters that are governed by the random market mode. In 1989, the regime-switching model was first introduced by Hamilton (1989) to describe a regime-switching time series. In option pricing, regime-switching model has been applied in various other problems. Zhang (2001) used this model to calculate an optimal selling rule and Yin and Zhang (1998) applied this in portfolio management. Also, Yin and Zhou (2003) studied a dynamic Markowitz problem for a market consisting of one bank account and multiple stocks.

In this study, we consider an efficient and accurate numerical method of a regime-switching model for European options (Kim, Jang, & Lee, 2008). Among several numerical methods for pricing of options with multi-underlying assets, the operator splitting (OS) scheme will be used: see Duffy (2006) and Ikonen and Toivanen (2004). In general, standard finite difference methods (FDM) do not work well for discrete options due to non-smooth payoffs or discontinuous derivatives at the exercise price. On the other hand, the OS scheme does not result in problematic oscillations due to the source term (Jeong & Kim, 2013). The main purpose of this paper is to observe the volatility smile and term structure of a regime-switching model by using an efficient and accurate numerical method. This work is an extension of the earlier one-dimensional study of Buffington and Elliott (2002).

This paper is organized as follows. In Section 2, we briefly introduce the risk-neutral valuation method and regime-switching.

☆ The first author (J.S. Kim) was supported by the National Institute for Mathematical Sciences (NIMS) grant funded by the Korea government (No. A21301). The corresponding author (D.H. Shin) was supported by Inha University and the Institute of Basic Science Korea University. The material in this paper was not presented at any conference. This paper was recommended for publication in revised form by Editor Berç Rüstem.

E-mail addresses: cfdkim@korea.ac.kr, tinayoyo@korea.ac.kr (J. Kim), dhshin@inha.ac.kr (D.-H. Shin).

1 Tel.: +82 2 3290 3077; fax: +82 2 929 8562.

2 Tel.: +82 32 860 7788; fax: +82 32 866 6877.

0005-1098/$ – see front matter © 2014 Elsevier Ltd. All rights reserved.
http://dx.doi.org/10.1016/j.automatica.2013.12.019

In Section 3, we discuss the Feynman–Kac type formula that is satisfied by the option valuation function. We describe the algorithm of the OS method for the formula at the end of this section. In Section 4, we perform convergence test and comparison study of ADI and OS methods. The volatility smile and term structure with a simple regime-switching model are reported in Section 5. In this section, we propose an algorithm for finding the implied volatility and by using this algorithm, we carry out several numerical parameter tests. We conclude this study in Section 6.

2. Risk neutral pricing

Standard research in derivative pricing follows the idea that the expected rate of return of all securities has the same risk-free interest rate in an appropriate probability space. We call the probability space the risk-neutral world, and the discount asset price is a martingale in this world.

Let $(\Omega, \mathcal{F}, P)$ denote the probability space and $\{\alpha(t)\}$ denote a continuous-time Markov chain with state space $\mathcal{M} = \{1, 2, \ldots, m\}$. In a regime-switching model, $\{\alpha(t)\}$ represents the market regime that determines the rate of return and volatility. Then, for example, the price of a stock $X(t)$ at time t is governed by:

$$dX(t) = X(t)\left[\mu(\alpha(t))dt + \sigma(\alpha(t))dw(t)\right], \quad \text{for } 0 \le t \le T, \qquad X(0) = X_0.$$

Let $Q = (q_{ij})_{m\times m}$ be the generator of $\alpha(t)$ with $q_{ij} \ge 0$ for $i \ne j$ and $\sum_{j\ne i}^m q_{ij} = -q_{ii}$ for each $i \in \mathcal{M}$. For any function f on $\mathcal{M}$, we denote $Qf(\cdot)(i) := \sum_{j=1}^m q_{ij} f(j)$.

In this paper, one of our objectives is to price European style options under regime-switching multi-underlying assets. Consider $X_k(t)$ as the price of stock k at time t with

$$dX_k(t) = X_k(t)\left[\mu_k(\alpha(t))dt + \sigma_k(\alpha(t))dw_k(t)\right], \quad \text{for } 0 \le t \le T,\ k = 1, 2, \ldots, d, \quad \text{and} \quad X_k(0) = X_{k0}, \tag{1}$$

where $\mu_k(i)$ and $\sigma_k(i)$ respectively represent the expected rate of return for X_k and the volatility of the stock price X_k at regime $i \in \mathcal{M}$, and $w_k(\cdot)$ denotes the standard Brownian motion. The Wiener processes are correlated by

$$\langle dw_k, dw_l\rangle = \rho_{kl}dt, \quad \text{for } \rho_{kl} \in [-1, 1].$$

In order to introduce derivative pricing in the risk neutral market, we also discuss the martingale measure characterized in Lemma 1. Assume that $X_0, \alpha(\cdot)$, and $w_k(\cdot)$ are mutually independent, and $\sigma_k^2(i) > 0$ for all $i \in M$. Let $\mathcal{F}_t$ denote the sigma field generated by $\{(\alpha(s), w_k(s)) : 0 \le s \le t\}$, and let $r > 0$ denote the risk-free rate. For $0 \le t \le T$, let

$$Z_t := \exp\left[\int_0^t \beta_k(s)dw_k(s) - \frac{1}{2}\int_0^t \beta_k^2(s)ds\right],$$

where

$$\beta_k(s) := \frac{r - \mu_k(\alpha(s))}{\sigma_k(\alpha(s))}.$$

Then, in lieu of Ito's rule,

$$\frac{dZ_t}{Z_t} = \beta_k(t)dw_k(t)$$

and Z_t is a local martingale with

$$E[Z_t] = 1, \quad 0 \le t \le T.$$

We define an equivalent measure $\widetilde{P}$ with the following

$$\frac{d\widetilde{P}}{dP} = Z_T.$$

Therefore Lemma 1 is a generalized Girsanov's theorem for Markov-modulated processes.

Lemma 1. *(1) Let $\widetilde{w}_k(t) := w_k(t) - \int_0^t \beta_k(s)\,ds (k = 1 : d)$. Then, $\widetilde{w}_k(t)$ is a $\widetilde{P}$-Brownian motion.*

(2) X_0, $\alpha(\cdot)$, and $\widetilde{w}_k(\cdot)$ are mutually independent under $\widetilde{P}$.

(3) Let $\mathbf{X}(t) := (X_1(t), X_2(t), \ldots, X_d(t))$, $c \le t$, and $\sigma_{X_k}(i) :=$ the volatility of stock X_k at regime i. Dynkin's formula holds: for any smooth function $\mathcal{F}(t, \mathbf{X}, i)$, we have

$$\mathcal{F}(t, \mathbf{X}(t), \alpha(t)) = \mathcal{F}(c, \mathbf{X}(c), \alpha(c)) + \int_c^t \mathcal{A}\mathcal{F}(s, \mathbf{X}(s), \alpha(s))ds + M(t) - M(c),$$

where $M(\cdot)$ is a $\widetilde{P}$-martingale and $\mathcal{A}$ is a generator given by

$$\begin{aligned}\mathcal{A}\mathcal{F} = {}& \frac{\partial}{\partial t}\mathcal{F}(t, \mathbf{X}, i) + \sum_{k=1}^d rX_k \frac{\partial}{\partial X_k}\mathcal{F}(t, \mathbf{X}, i)\\ &+ \frac{1}{2}\sum_{k=1}^d\sum_{l=1}^d \rho_{kl}(i)\sigma_{X_k}(i)\sigma_{X_l}(i)X_kX_l\frac{\partial^2}{\partial X_k\partial X_l}\mathcal{F}(t, \mathbf{X}, i)\\ &+ Q\mathcal{F}(t, \mathbf{X}, \cdot)(i),\end{aligned}$$

where $\rho_{kk} = 1$ for $1 \le k \le d$.

Proof. See Chapter 14 in Yao, Zhang, and Zhou (2006). □

From Lemma 1 and this point of view of Fouque, Papanicolaou, and Sircar (2000) and Hull (2000), $(\Omega, \mathcal{F}, \{\mathcal{F}_t\}, \widetilde{P})$ defines a risk-neutral world. And $e^{-rt}X(t)$ is a $\widetilde{P}$-martingale.

3. A numerical approach with OS methods

In this paper, we consider European style option pricing under two regime-switching underlying assets $X_1(t)$ and $X_2(t)$. Let $x := X_1(t)$, $y := X_2(t)$, and $\mathbf{U}(x, y, t, i)$ be the values of a European style call option with two underlying assets with regime i for $i = 1, 2$. Using a Feynman–Kac formula, a partial difference equation with respect to $\mathbf{U}(x, y, t) = (u(x, y, t), v(x, y, t))^T$ is derived as follows:

$$\frac{\partial \mathbf{U}}{\partial t} + rx\frac{\partial \mathbf{U}}{\partial x} + ry\frac{\partial \mathbf{U}}{\partial y} - r\mathbf{U} + \frac{1}{2}(\sigma_x x)^2\frac{\partial^2\mathbf{U}}{\partial x^2} + \frac{1}{2}(\sigma_y y)^2\frac{\partial^2\mathbf{U}}{\partial y^2} + \rho_{xy}\sigma_x\sigma_y xy\frac{\partial^2\mathbf{U}}{\partial x\partial y} + Q\mathbf{U} = 0,$$

where $Q = \begin{pmatrix} -\lambda^u & \lambda^u \\ \lambda^v & -\lambda^v \end{pmatrix}$ and λ^u, λ^v represent jumping rates for u and v, respectively.

Then, by each component of $\mathbf{U}$, we have the following system:

$$\begin{aligned}&\frac{\partial u}{\partial t} + r^u x\frac{\partial u}{\partial x} + r^u y\frac{\partial u}{\partial y} - r^u u + \frac{1}{2}(\sigma_x^u x)^2\frac{\partial^2 u}{\partial x^2} + \frac{1}{2}(\sigma_y^u y)^2\frac{\partial^2 u}{\partial y^2}\\ &\quad + \rho_{xy}^u\sigma_x^u\sigma_y^u xy\frac{\partial^2 u}{\partial x\partial y} + \lambda^u(v - u) = 0,\end{aligned} \tag{2}$$

$$\begin{aligned}&\frac{\partial v}{\partial t} + r^v x\frac{\partial v}{\partial x} + r^v y\frac{\partial v}{\partial y} - r^v v + \frac{1}{2}(\sigma_x^v x)^2\frac{\partial^2 v}{\partial x^2} + \frac{1}{2}(\sigma_y^v y)^2\frac{\partial^2 v}{\partial y^2}\\ &\quad + \rho_{xy}^v\sigma_x^v\sigma_y^v xy\frac{\partial^2 v}{\partial x\partial y} + \lambda^v(u - v) = 0.\end{aligned} \tag{3}$$

The terminal conditions $u(x, y, T) = v(x, y, T)$ are given by $\Lambda(x, y)$.

3.1. Discretization

Let $\mathcal{L}_u(u)$ be the operator value as

$$\mathcal{L}_u(u) = r^u x\frac{\partial u}{\partial x} + r^u y\frac{\partial u}{\partial y} - r^u u + \frac{1}{2}(\sigma_x^u x)^2\frac{\partial^2 u}{\partial x^2} + \frac{1}{2}(\sigma_y^u y)^2\frac{\partial^2 u}{\partial y^2} + \rho_{xy}^u\sigma_x^u\sigma_y^u xy\frac{\partial^2 u}{\partial x\partial y} + \lambda^u(v-u). \quad (4)$$

Then Eq. (2) can be written as

$$\frac{\partial u}{\partial \tau} = \mathcal{L}_u(u) \quad \text{for } (x, y, \tau) \in \Omega \times [0, T],$$

where $\tau = T - t$. Eq. (3) can be written easily by using operator $\mathcal{L}_v$ as in $\partial v/\partial\tau = \mathcal{L}_v(v)$.

In the computational domain $\Omega = (0, L) \times (0, M)$, we use the Dirichlet boundary conditions at $x = L$ and $y = M$ and the linear boundary conditions at $x = 0$ and $y = 0$. Similarly, the linear boundary conditions are applied to v.

3.2. Operator splitting method (OSM)

The operator splitting (OS) scheme is used extensively in mathematical finance for solving multi-asset option pricing models numerically. The idea of the OS method (Duffy, 2006) is to divide each time step into fractional time steps with simpler operators. We shall introduce the basic idea behind the OS method, which is to replace a two-dimensional scheme as

$$\frac{u_{ij}^{n+1} - u_{ij}^n}{\Delta\tau} = \mathcal{L}_u^x\left(u_{ij}^*\right) + \mathcal{L}_u^y\left(u_{ij}^{n+1}\right),$$

$$\frac{v_{ij}^{n+1} - v_{ij}^n}{\Delta\tau} = \mathcal{L}_v^x\left(v_{ij}^*\right) + \mathcal{L}_v^y\left(v_{ij}^{n+1}\right),$$

where u^* and v^* are values at an intermediate time level $*$ which is between time level n and $n+1$ and the discrete difference operator $\mathcal{L}_u^x$. And $\mathcal{L}_u^y$ are defined by

$$\begin{aligned}\mathcal{L}_u^x\left(u_{ij}^*\right) = {} & r^u x_i\frac{u_{i+1,j}^* - u_{ij}^*}{h} - \frac{1}{2}r^u u_{ij}^* \\ & + \frac{1}{2}(\sigma_x^u x_i)^2\frac{u_{i-1,j}^* - 2u_{ij}^* + u_{i+1,j}^*}{h^2} \\ & + \frac{1}{2}\rho_{xy}^u\sigma_x^u\sigma_y^u x_i y_j\frac{u_{i+1,j+1}^n + u_{ij}^n - u_{i,j+1}^n - u_{i+1,j}^n}{h^2} \\ & + \frac{1}{2}\lambda^u(v_{ij}^n - u_{ij}^*),\end{aligned}$$

$$\begin{aligned}\mathcal{L}_u^y\left(u_{ij}^{n+1}\right) = {} & r^u y_j\frac{u_{ij+1}^{n+1} - u_{ij}^{n+1}}{h} - \frac{1}{2}r^u u_{ij}^{n+1} \\ & + \frac{1}{2}(\sigma_y^u y_j)^2\frac{u_{ij-1}^{n+1} - 2u_{ij}^{n+1} + u_{ij+1}^{n+1}}{h^2} \\ & + \frac{1}{2}\rho_{xy}^u\sigma_x^u\sigma_y^u x_i y_j\frac{u_{i+1,j+1}^* + u_{ij}^* - u_{ij+1}^* - u_{i+1,j}^*}{h^2} \\ & + \frac{1}{2}\lambda^u(v_{ij}^n - u_{ij}^{n+1}).\end{aligned}$$

Here, we apply the implicit scheme for time derivative and the mixed scheme for space derivatives which is forward for first order derivatives and central for second order derivative. In order to deal with non-derivative terms in each step, we split evenly the non-derivative terms. And the remaining operators $\mathcal{L}_v^x$ and $\mathcal{L}_v^y$ are defined similarly as the operators $\mathcal{L}_u^x$ and $\mathcal{L}_u^y$.

Then, we approximate each sub-problem by a semi-implicit scheme as

$$\frac{u_{ij}^* - u_{ij}^n}{\Delta\tau} = \mathcal{L}_u^x\left(u_{ij}^*\right), \quad (5)$$

$$\frac{u_{ij}^{n+1} - u_{ij}^*}{\Delta\tau} = \mathcal{L}_u^y\left(u_{ij}^{n+1}\right), \quad (6)$$

$$\frac{v_{ij}^* - v_{ij}^n}{\Delta\tau} = \mathcal{L}_v^x\left(v_{ij}^*\right), \quad (7)$$

$$\frac{v_{ij}^{n+1} - v_{ij}^*}{\Delta\tau} = \mathcal{L}_v^y\left(v_{ij}^{n+1}\right). \quad (8)$$

We describe a numerical algorithm based on an operator splitting method for the governing Eqs. (5)–(8).

- *Step* 1

Eq. (5) is rewritten as follows:

$$\alpha_i u_{i-1,j}^* + \beta_i u_{ij}^* + \gamma_i u_{i+1,j}^* = f_{ij}. \quad (9)$$

With a fixed index j and for $i = 1 : N_x$, the vector $u_{1:N_x,j}^*$ can be found by solving the tridiagonal system

$$A_x u_{1:N_x,j}^* = f_{1:N_x,j},$$

where A_x is a tridiagonal matrix constructed from Eq. (9) with the Dirichlet and linear boundary conditions, i.e.,

$$A_x = \begin{pmatrix} 2\alpha_1 + \beta_1 & \gamma_1 + \alpha_1 & 0 & \cdots & 0 & 0 \\ \alpha_2 & \beta_2 & \gamma_2 & \cdots & 0 & 0 \\ 0 & \alpha_3 & \beta_3 & \cdots & 0 & 0 \\ \vdots & \vdots & \vdots & \ddots & \vdots & \vdots \\ 0 & 0 & 0 & \cdots & \beta_{N_x-1} & \gamma_{N_x-1} \\ 0 & 0 & 0 & \cdots & \alpha_{N_x} & \beta_{N_x} - \gamma_{N_x} \end{pmatrix}.$$

Here, the elements of the matrix A_x are

$$\alpha_i = -\frac{(\sigma_x^u x_i)^2}{2h^2}, \quad (10)$$

$$\beta_i = \frac{1}{\Delta\tau} + \frac{(\sigma_x^u x_i)^2}{h^2} + \frac{r^u x_i}{h} + \frac{1}{2}(r^u + \lambda^u), \quad (11)$$

$$\gamma_i = -\frac{(\sigma_x^u x_i)^2}{2h^2} - \frac{r^u x_i}{h}, \quad \text{for } i = 1 : N_x. \quad (12)$$

For given the u_{ij}^n, the elements of the vector $f_{1:N_x,j}$ are

$$\begin{aligned} f_{ij} = {} & \frac{u_{ij}^n}{\Delta\tau} + \frac{1}{2}\lambda^u v_{ij}^n \\ & + \frac{1}{2}\rho_{xy}^u\sigma_x^u\sigma_y^u\frac{u_{i+1,j+1}^n + u_{ij}^n - u_{i,j+1}^n - u_{i+1,j}^n}{h^2}, \\ & \text{for } i = 1 : N_x. \end{aligned} \quad (13)$$

Then, the first step of the governing equation is implemented in a loop over the y-direction as follows:

Algorithm 1 (Step 1)

Require: Previous data u^n, v^n.
  procedure FIND THE SOLUTION u^*
    for $j = 1; j \le N_y; j{+}{+}$ **do**
      for $i = 1; i \le N_x; i{+}{+}$ **do**
        Set α_i, β_i, γ_i, and f_{ij} by Eqs. (10)–(13)
      end for
      Solve $A_x u_{1:N_x,j}^* = f_{1:N_x,j}$
        by using the Thomas algorithm
    end for
  end procedure

- *Step* 2

The second step which is given by Eq. (6) is rewritten as

$$\alpha_j u^{n+1}_{ij-1} + \beta_j u^{n+1}_{ij} + \gamma_j u^{n+1}_{ij+1} = g_{ij}, \tag{14}$$

for given the u^*_{ij} and where

$$\alpha_j = -\frac{(\sigma^u_y y_j)^2}{2h^2}, \tag{15}$$

$$\beta_j = \frac{1}{\Delta\tau} + \frac{(\sigma^u_y y_j)^2}{h^2} + \frac{r^u y_j}{h} + \frac{1}{2}(r^u + \lambda^u), \tag{16}$$

$$\gamma_j = -\frac{(\sigma^u_y y_j)^2}{2h^2} - \frac{r^u y_j}{h}, \tag{17}$$

$$g_{ij} = \frac{u^*_{ij}}{\Delta\tau} + \frac{1}{2}\lambda^u v^n_{ij} + \frac{1}{2}\rho^u_{xy}\sigma^u_x\sigma^u_y \frac{u^n_{i+1,j+1} + u^n_{ij} - u^n_{i,j+1} - u^n_{i+1,j}}{h^2}. \tag{18}$$

For a fixed index i and for $j = 1 : N_y$, the vector $u^{n+1}_{i,1:N_y}$ can be found by solving the tridiagonal system

$A_y u^{n+1}_{i,1:N_y} = g_{i,1:N_y}$,

where the matrix A_y is a tridiagonal, i.e.,

$$A_y = \begin{pmatrix} 2\alpha_1+\beta_1 & \gamma_1+\alpha_1 & 0 & \cdots & 0 & 0 \\ \alpha_2 & \beta_2 & \gamma_2 & \cdots & 0 & 0 \\ 0 & \alpha_3 & \beta_3 & \cdots & 0 & 0 \\ \vdots & \vdots & \vdots & \ddots & \vdots & \vdots \\ 0 & 0 & 0 & \cdots & \beta_{N_y-1} & \gamma_{N_y-1} \\ 0 & 0 & 0 & \cdots & \alpha_{N_y} & \beta_{N_y}-\gamma_{N_y} \end{pmatrix}.$$

The second step of the governing equation is implemented in a loop over the x-direction as follows:

Algorithm 2 (Step 2)

Require: Previous data u^*, v^n.
  procedure FIND THE SOLUTION u^{n+1}
    for $i = 1; j \le N_x; i{+}{+}$ **do**
      for $j = 1; j \le N_y; j{+}{+}$ **do**
        Set α_j, β_j, γ_j, and g_{ij} by Eqs. (15)–(18)
      end for
      Solve $A_y u^{n+1}_{i,1:N_y} = g_{i,1:N_y}$
        by using the Thomas algorithm
    end for
  end procedure

As with *Steps* 1 and 2, the third and fourth steps are implemented by using Eqs. (7) and (8), respectively. Here, the description for *Steps* 3 and 4 will be omitted because it follows a similar process.

- Execution from *Steps* 1 to 4 advances the numerical solution with a $\Delta\tau$ step in time.

4. Numerical experiments

We consider a vanilla call option whose payoff is given as

$$\Lambda(x, y) = \max\{x - K_1, y - K_2, 0\}. \tag{19}$$

Fig. 1 shows the payoff function (19).

The parameters used are $K_1 = K_2 = 50$, $\sigma^u_x = 0.3$, $\sigma^v_x = 0.8$, $\sigma^u_y = \sigma^v_y = 0.3$, $\rho^u_{xy} = \rho^v_{xy} = 0.5$, $r^u = r^v = 0.05$, $T = 0.5$. The computational domain is $[0, 150] \times [0, 150]$ with space step

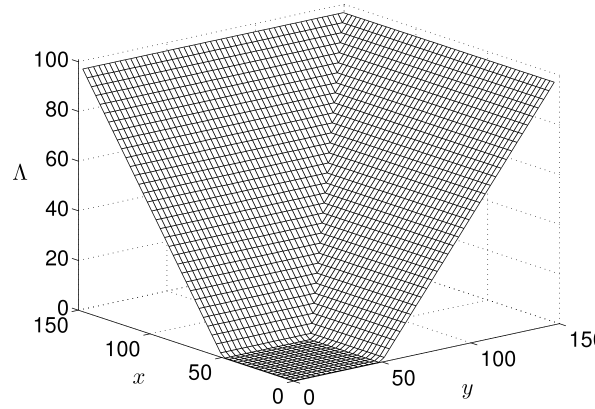

Fig. 1. European call option payoff on the maximum of two assets.

$N_x = N_y = 150$. And we set $\lambda^u = 0.0$, $\lambda^v = 4.0$ which means that regime state $i = 1$ is an absorbing state.

Fig. 2(a) and (b) shows the value function of u, which has no regime-switching until the total time $T = 0.5$, and v, which has at most one regime-switching during the life time of the option, under the operator splitting scheme with 50 time steps per 0.5 year. And Fig. 2(c) represents the difference between u and v which comes from the probability of change in the x-asset volatility σ_x.

4.1. Convergence test

In this section, we perform a number of simulations with increasingly finer grids $h = 3/2^n$ for $n = 0, 1, 2$, and 3 on a computational domain $\Omega = [0, 150] \times [0, 150]$. For each case, the calculation is run up to time $T = 0.5$ with time step $\Delta\tau = 0.01/4^n$. The initial conditions for u and v are taken as maximum option payoff as shown in Fig. 1.

Since there is no closed-form analytic solution for this problem, we use the Richardson method. We define the error of a grid as the discrete l_2-norm of the difference between that grid and the average of the reference solution cell neighboring it as

$$e_{h/\frac{h}{2}\,ij} := v_{h_{ij}} - \left(v_{\frac{h}{2}\,2i-1,2j-1} + v_{\frac{h}{2}\,2i,2j-1} + v_{\frac{h}{2}\,2i-1,2j} + v_{\frac{h}{2}\,2i,2j}\right)/4.$$

The rate of convergence is defined as the ratio of successive errors which is $\log_2\left(\|e_{h/\frac{h}{2}}\|_2 / \|e_{\frac{h}{2}/\frac{h}{4}}\|_2\right)$. The errors and rates of convergence obtained using these definitions are given in Table 1. First-order accuracy with respect to space is observed, as expected from the discretization.

4.2. Comparison between ADI and OS methods

In order to highlight why OS method can be particularly useful in regime-switching model, we compare standard ADI (Alternating Directions Implicit) method with OS methods. Before we do this, we explain briefly about ADI method.

The main idea of the ADI method (Chin, Manteuffel, & Pillis, 1984; Hout & Foulon, 2010) is to proceed in two steps, treating only one operator implicitly at each stage. First, a half-step is taken implicitly in x and explicitly in y. Then, the other half-step is taken implicitly in y and explicitly in x. The followings are the applied scheme to Eq. (2) as

$$\frac{u^*_{ij} - u^n_{ij}}{\Delta\tau} = \mathcal{L}^x_{ADI}\left(u^*_{ij}\right), \tag{20}$$

$$\frac{u^{n+1}_{ij} - u^*_{ij}}{\Delta\tau} = \mathcal{L}^y_{ADI}\left(u^{n+1}_{ij}\right), \tag{21}$$

Table 1
Errors and rates of convergence for numerical solution u.

Case	50–100	Rate	100–200	Rate	200–400
l_2-error	0.0299	1.12	0.0137	1.05	0.0067

where the discrete difference operators $\mathcal{L}^x_{ADI}$ and $\mathcal{L}^y_{ADI}$ are defined by

$$\begin{aligned}\mathcal{L}^x_{ADI}\left(u^*_{ij}\right) = {} & \frac{1}{2}r^u x_i \frac{u^*_{i+1,j}-u^*_{ij}}{h} + \frac{1}{2}r^u y_j \frac{u^n_{ij+1}-u^n_{ij}}{h} \\ & - \frac{1}{2}r^u u^*_{ij} + \frac{1}{4}(\sigma^u_x x_i)^2 \frac{u^*_{i+1,j}-2u^*_{ij}+u^*_{i-1,j}}{h^2} \\ & + \frac{1}{4}(\sigma^u_y y_j)^2 \frac{u^n_{i,j+1}-2u^n_{ij}+u^n_{i,j-1}}{h^2} \\ & + \frac{1}{2}\rho^u_{xy}\sigma^u_x\sigma^u_y x_i y_j \frac{u^n_{i+1,j+1}+u^n_{ij}-u^n_{ij+1}-u^n_{i+1,j}}{h^2} \\ & + \frac{1}{2}\lambda^u (v^n_{ij}-u^*_{ij}), \end{aligned} \tag{22}$$

$$\begin{aligned}\mathcal{L}^y_{ADI}\left(u^{n+1}_{ij}\right) = {} & \frac{1}{2}r^u x_i \frac{u^*_{i+1,j}-u^*_{ij}}{h} + \frac{1}{2}r^u y_j \frac{u^{n+1}_{ij+1}-u^{n+1}_{ij}}{h} \\ & - \frac{1}{2}r^u u^{n+1}_{ij} + \frac{1}{4}(\sigma^u_x x_i)^2 \frac{u^*_{i+1,j}-2u^*_{ij}+u^*_{i-1,j}}{h^2} \\ & + \frac{1}{4}(\sigma^u_y y_j)^2 \frac{u^{n+1}_{i,j+1}-2u^{n+1}_{ij}+u^{n+1}_{i,j-1}}{h^2} \\ & + \frac{1}{2}\rho^u_{xy}\sigma^u_x\sigma^u_y x_i y_j \frac{u^*_{i+1,j+1}+u^*_{ij}-u^*_{ij+1}-u^*_{i+1,j}}{h^2} \\ & + \frac{1}{2}\lambda^u (v^n_{ij}-u^{n+1}_{ij}). \end{aligned} \tag{23}$$

Here, u^* is the value at an intermediate time level $*$ which is between time level n and $n+1$. Similar to Eqs. (20) and (21), Eq. (3) is applied with ADI method for v.

Fig. 3 shows numerical results using the ADI and OS methods with $\Delta\tau = 0.5$ and $h = 1$. The first and second columns are results with solutions v^* and v^1, respectively. Here, v^1 is the numerical solution at time $T = \Delta\tau$ after one iteration. And v^* is the value at an intermediate time level between v^0 and v^1. In Fig. 3(a), the solution v^* exhibits oscillation around $y = K_2$ which is from the y-derivatives in the source term. On the other hand, for the OS method, we do not have the y-derivatives in the source term and the solution $v^{\frac{1}{2}}$ is smooth around $y = K_2$ as shown in Fig. 3(b). After one complete time step, the result with the ADI shows a non-smooth numerical solution. However, the OS method results in a smooth numerical solution. Therefore, the results showed that the OS method is very efficient and robust than the ADI method with large time steps. For more details, see the texts of Jeong and Kim (2013).

5. Volatility smile and volatility term structure

In this section, we discuss the volatility smile phenomenon generated by the regime-switching model. We illustrate the volatility smile and the term structure for the case of two-underlying assets with payoff function (19).

Since the volatility smile can be described for a simple case, we especially focus on a special case of the regime-switching model that has two states with one absorbing state; Q is given by

$$Q = \begin{pmatrix} 0 & 0 \\ \lambda & -\lambda \end{pmatrix}$$

with $\lambda > 0$.

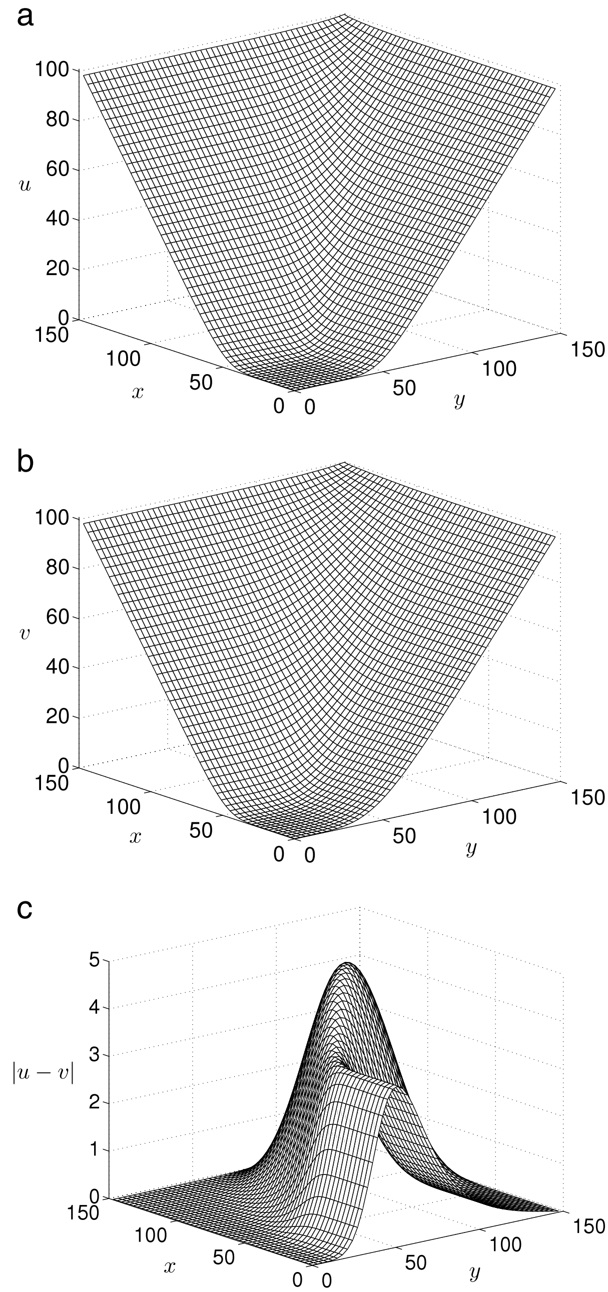

Fig. 2. Numerical results using the OS method with European call option on the maximum of two assets at $T = 0.5$. (a) Numerical solution u, (b) numerical solution v, and (c) difference between $|u - v|$.

5.1. Algorithm of implied volatility

Following Algorithm 3 is for finding the implied volatility. To find the implied volatility σ_{imp} on the interval $[\sigma_{\text{low}}, \sigma_{\text{high}}]$, we first need the numerical solution v for regime-switching model with given parameter set. Then, by computing the numerical value at the midpoint $0.5(\sigma_{\text{low}}+\sigma_{\text{high}})$, we can find the implied volatility. In this case, the numerical values for the bisection method are calculated numerically with the Black–Scholes model because $\lambda^u = 0$ means the classical Black–Scholes part which is with no jump.

5.2. Numerical simulation for implied volatility

In this section, we perform numerical simulations for implied volatility on a computational domain $\Omega = [0, 150] \times [0, 150]$ with space step $h = 1$ and time step $\Delta\tau = 0.0025$.

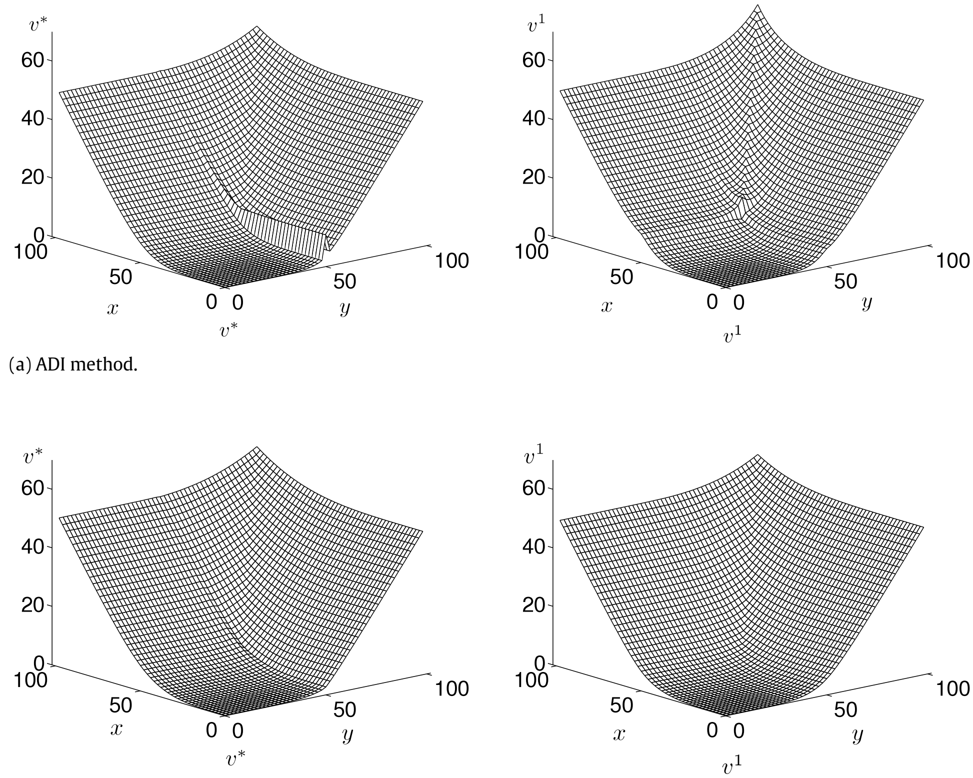

(a) ADI method.

(b) OS method.

Fig. 3. Numerical results using the (a) ADI and (b) OS methods with European call option on the maximum of two assets. First and second columns represent the solution v^* and v^1, respectively.

Algorithm 3 Bisection method for finding implied volatility

Require: Previous data v; endpoints σ_{low} and σ_{high}; tolerance *tol*.

procedure FIND THE IMPLIED VOLATILITY

  Set $\sigma_{\text{imp}} = 0.5(\sigma_{\text{low}} + \sigma_{\text{high}})$ and $i = 0$.

  while $|\sigma_{\text{high}} - \sigma_{\text{imp}}| > tol$ **do**

    $i = i + 1$.

    $P_{\text{high}} =$ **Numerical OSM**(σ_{high}).

    $P_{\text{imp}} =$ **Numerical OSM**(σ_{imp}).

    if $(P_{\text{imp}} - v)(P_{\text{high}} - v) \le 0$ **then**

      $\sigma_{\text{low}} = \sigma_{\text{imp}}$.

    else

      $\sigma_{\text{high}} = \sigma_{\text{imp}}$.

    end if

    $\sigma_{\text{imp}} = 0.5(\sigma_{\text{low}} + \sigma_{\text{high}})$.

  end while

end procedure

The following numerical parameters are used to illustrate the volatility smile in our model.

$\Omega_{K_x} = \{30, 35, \ldots, 70\}$,

$\Omega_{K_y} = \{30, 35, \ldots, 70\}$,

$\Omega_T = \left\{\frac{1}{12}, \frac{2}{12}, \ldots, 1\right\}$,

$\Omega_\lambda = \{2, 4, \ldots, 20\}$,

$\Omega_\rho = \{-0.8, -0.6, \ldots, 0.8\}$,

$\Omega_\sigma = \{0.1, 0.2, \ldots, 1\}$,

where, in particular, Ω_σ is the set of volatility jump sizes $|\sigma_x^v - \sigma_x^u| \in \Omega_\sigma$. In all cases, we set $r^u = r^v = 0.05$, $\sigma_y^u = \sigma_y^v = 0.3$, $K_y = 50$, $\rho_{xy}^v = 0.5$, $\lambda^u = 0$, and $x = y = 50$ while varying other parameters. We calculate the implied volatilities about the variable strike price for x-asset K_x against one of the other parameters K_y, T, λ^v, σ_x^u, σ_x^v, and ρ_{xy}^u.

5.2.1. K_x and K_y

As shown in Fig. 4, we estimate the implied volatility about v under the varying parameters $K_x \in \Omega_{K_x}$, $K_y \in \Omega_{K_y}$. We consider two different cases with $\sigma_x^u > \sigma_x^v$ and $\sigma_x^u < \sigma_x^v$ in Fig. 4(a) and (b), respectively.

In Fig. 4(a), we use the fixed parameters $(T, \lambda^v, \sigma_x^u, \sigma_x^v, \rho_{xy}^u) = (0.25, 4, 0.8, 0.3, 0.5)$. And in the other case (b), we set the fixed parameters $(T, \lambda^v, \sigma_x^u, \sigma_x^v, \rho_{xy}^u) = (0.25, 4, 0.3, 0.8, 0.5)$.

As the same volatility smile phenomenon in Hull (2000), the implied volatility reaches its minimum at $K_x = 50$ and $K_y = 50$ (at the money) and increases as K_x and K_y move away from 50.

Note that we do not use any practical option pricing data and that the option pricing values arise purely from our two-state continuous-time Markov regime-switching model.

5.2.2. K_x and T

In this example, we set $(K_y, \lambda^v, \rho_{xy}^u) = (50, 4, 0.5)$ and vary $K_x \in \Omega_{K_x}$ against $T \in \Omega_T$.

For the first case which is $\sigma_x^u > \sigma_x^v$, we take $\sigma_x^u = 0.8$, $\sigma_x^v = 0.3$. As the result, Fig. 5(a) shows that for each fixed $T \in \Omega_T$, the implied volatility reaches its minimum at $K_x = 50$ (at the money) and increase as K_x moves away from $K_x = 50$. In addition, for fixed $K_x \in \Omega_{K_x}$, the implied volatility is increasing in T, corresponding to a jump from σ_x^v to σ_x^u.

On the contrary to Fig. 5(a), (b) represents the implied volatility when $\sigma_x^u < \sigma_x^v$. For this, we use $\sigma_x^u = 0.3$, $\sigma_x^v = 0.8$. In this case, we can see that the implied volatility is decreasing in T, corresponding to a jump from σ_x^v to σ_x^u.

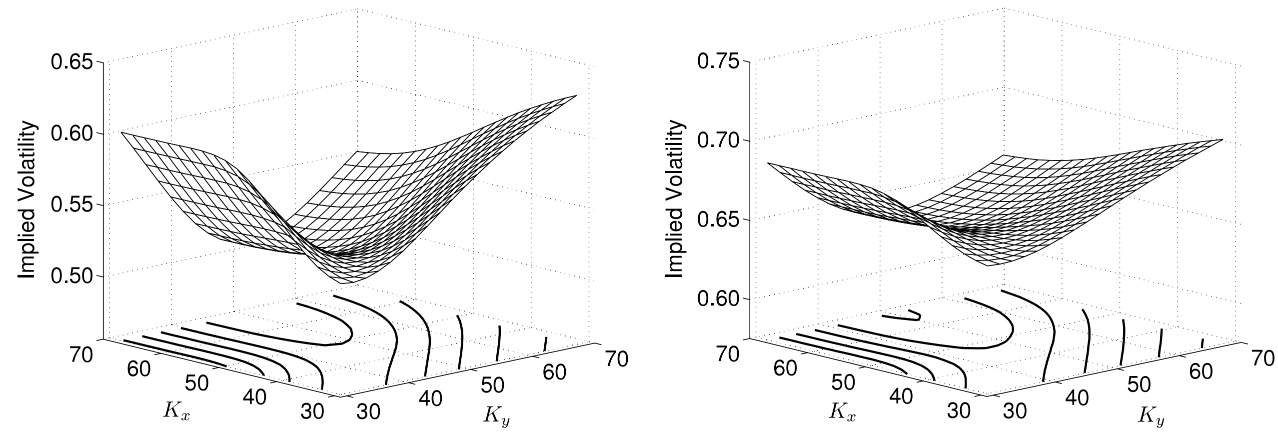

(a) $\sigma_x^u > \sigma_x^v$.

(b) $\sigma_x^u < \sigma_x^v$.

Fig. 4. Volatility smile and the term structure under the varying parameters K_x and K_y.

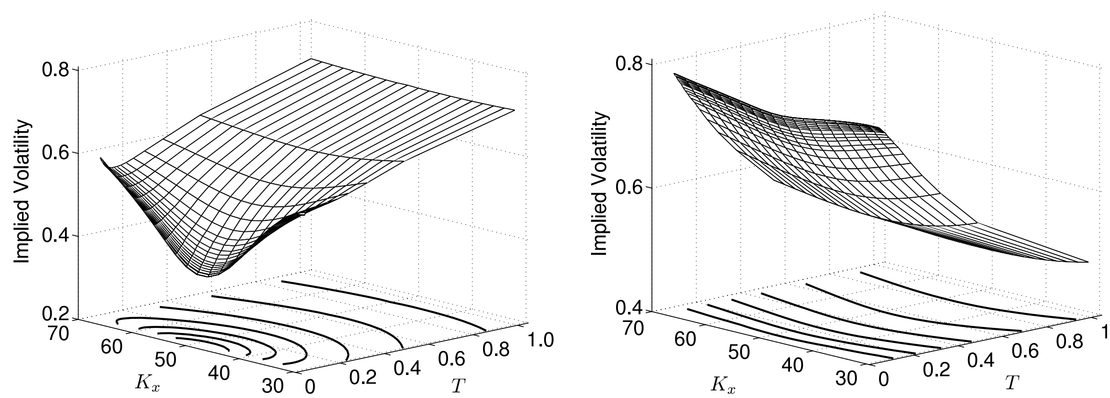

(a) $\sigma_x^u > \sigma_x^v$.

(b) $\sigma_x^u < \sigma_x^v$.

Fig. 5. Volatility smile and the term structure under the varying parameters K_x and T.

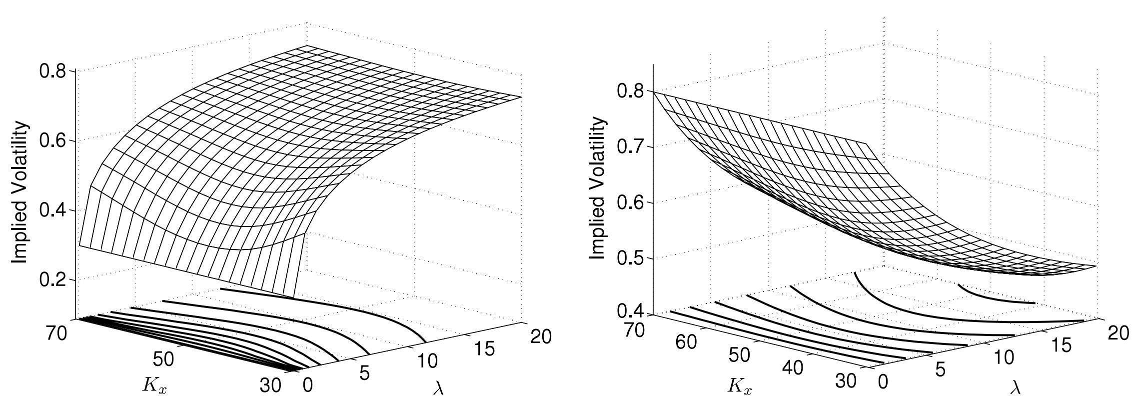

(a) $\sigma_x^u > \sigma_x^v$.

(b) $\sigma_x^u < \sigma_x^v$.

Fig. 6. Volatility smile and the term structure under the varying parameters K_x and λ.

5.2.3. K_x and λ

Then, we set $(K_y, T, \lambda^v, \rho_{xy}^u) = (50, 0.25, 4, 0.5)$ and vary $K_x \in \Omega_{K_x}$ versus $\lambda^u \in \Omega_\lambda$.

For the first case, we set $\sigma_x^u = 0.8, \sigma_x^v = 0.3$. As shown in Fig. 6(a), a large λ^u forces the implied volatility around σ_x^u for each fixed $K_x \in \Omega_{K_x}$.

For the second case which is $\sigma_x^u < \sigma_x^v$, we take $\sigma_x^u = 0.3, \sigma_x^v = 0.8$. Fig. 6(b) shows that for fixed $K_x \in \Omega_{K_x}$, the implied volatility decreases in larger λ^u.

5.2.4. K_x and σ

To obtain the numerical results in Fig. 7, we set $(K_y, T, \lambda^v, \rho_{xy}^u) = (50, 0.25, 4, 0.5)$ and vary $K_x \in \Omega_{K_x}$ versus $\sigma \in \Omega_\sigma$.

In the first case, we take that σ_x^u is varied from 0.3 to 1.3 when σ_x^v is fixed at 0.3. As can be seen from Fig. 7(a), the smile increases in the jump size. In addition, the implied volatility is an increasing function of $\sigma_x^u - \sigma_x^v$ for each fixed $K_x \in \Omega_{K_x}$.

Alternatively in the second case, we set $\sigma_x^u = 0.3$ and vary σ_x^v from 0.3 to 1.3 by the volatility jump size $\sigma_x^v - \sigma_x^u \in \Omega_\sigma$. As shown in Fig. 7(b), this result is similar to case (a).

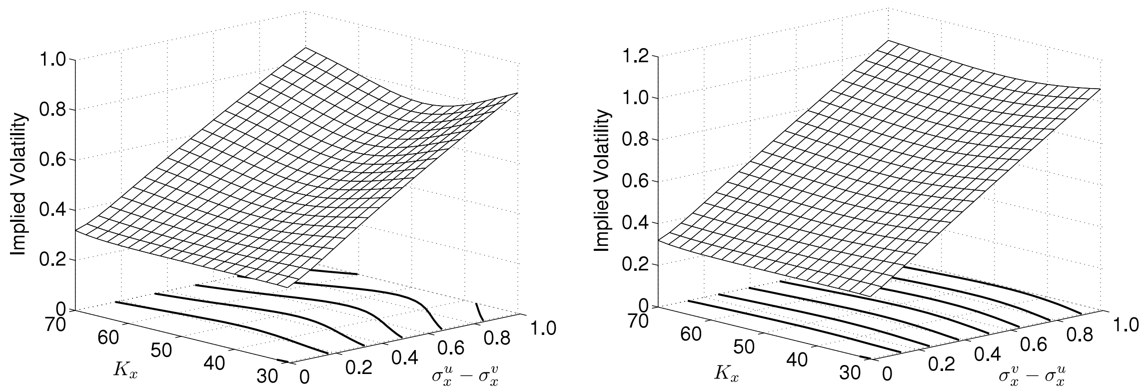

(a) $\sigma_x^u > \sigma_x^v$.

(b) $\sigma_x^u < \sigma_x^v$.

Fig. 7. Volatility smile and the term structure under the varying parameters K_x and σ.

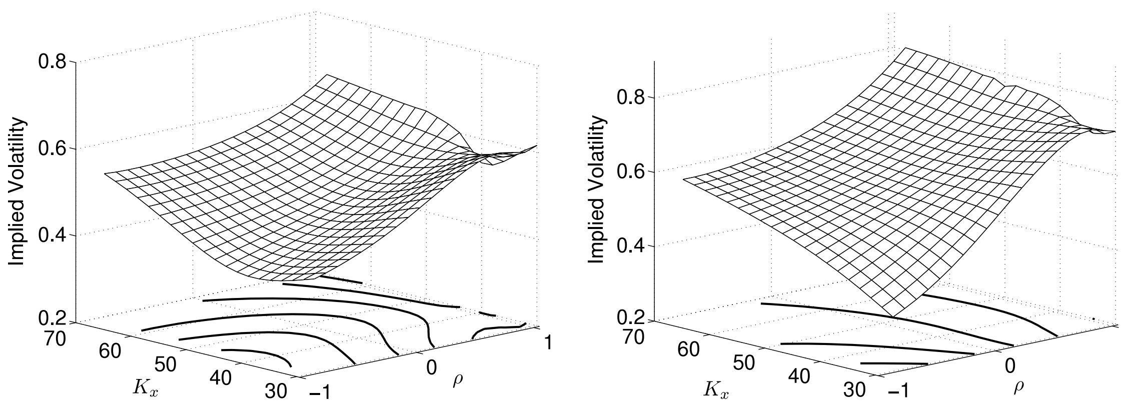

(a) $\sigma_x^u > \sigma_x^v$.

(b) $\sigma_x^u < \sigma_x^v$.

Fig. 8. Volatility smile and the term structure under the varying parameters K_x and ρ.

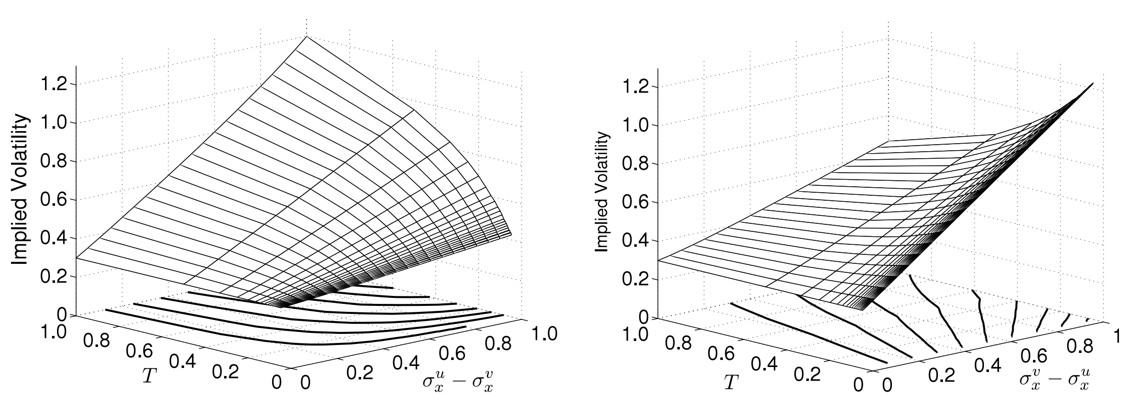

(a) $\sigma_x^u > \sigma_x^v$.

(b) $\sigma_x^u < \sigma_x^v$.

Fig. 9. Volatility smile and the term structure under the varying parameters T and σ.

5.2.5. K_x and ρ

Now, we set $(K_y, T, \lambda^v) = (50, 0.25, 4)$, $K_x \in \Omega_{K_x}$, and $\rho_{xy}^u \in \Omega_\rho$. And we take $(\sigma_x^u, \sigma_x^v) = (0.8, 0.3)$ for case (a), $(\sigma_x^u, \sigma_x^v) = (0.3, 0.8)$ for the other case (b). The numerical results are illustrated in Fig. 8. The volatility tend to increase as ρ_{xy}^u approaches to 1 for each fixed K_x.

5.2.6. T and σ

Here, we fix $(K_x, K_y, T, \lambda^v, \rho_{xy}^u) = (50, 50, 0.25, 4, 0.5)$ and we plot the implied volatility against the maturity T and the jump size $|\sigma_x^u - \sigma_x^v|$ in Fig. 9.

As can be observed in Fig. 9(a), we consider the case of $\sigma_x^u - \sigma_x^v$. For this, we fix $\sigma_x^v = 0.3$ and vary σ_x^u from 0.3 to 1.3. As a result, the implied volatility increases in T and $\sigma_x^u - \sigma_x^v$.

In the other case, we set $\sigma_x^u = 0.3$ and vary σ_x^v from 0.3 to 1.3. In Fig. 9(b), we can see that implied volatility decreases in T and $\sigma_x^u - \sigma_x^v$.

5.2.7. T and λ

As the final example, we consider the implied volatility against the maturity T and the jump rate λ^v as shown in Fig. 10. To do this, we take $(K_x, K_y, \rho_{xy}^u) = (50, 50, 0.5)$.

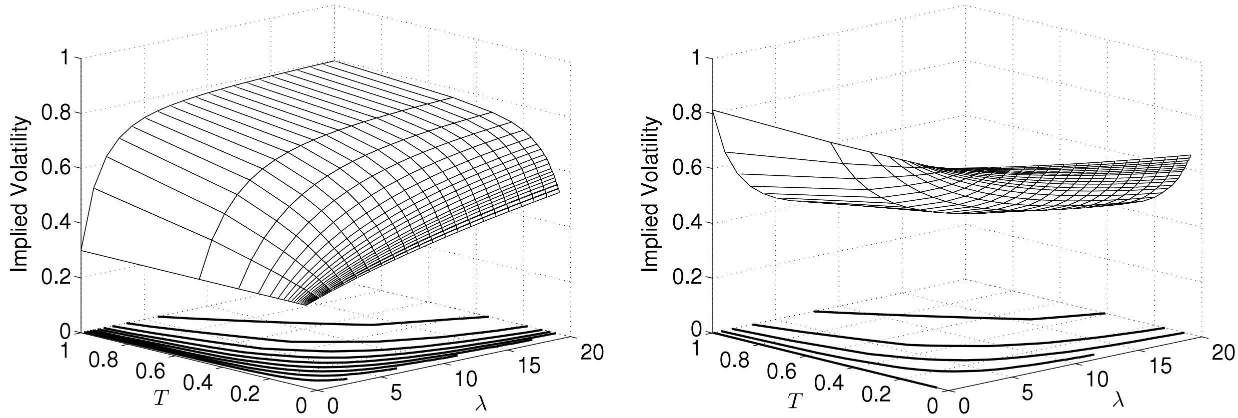

(a) $\sigma_x^u > \sigma_x^v$.   (b) $\sigma_x^u < \sigma_x^v$.

Fig. 10. Volatility smile and the term structure under the varying parameters T and λ.

For the first case when $\sigma_x^u > \sigma_x^v$, we set $\sigma_x^u = 0.8$ and $\sigma_x^v = 0.3$. Then, we can observe that for fixed T, the implied volatility increases in λ. Similarly, for fixed λ, the implied volatility also increase in T.

For the other case, we set $\sigma_x^u = 0.3$ and $\sigma_x^v = 0.8$. Then we can see that the implied volatility decreases in λ when T and λ are increased.

6. Conclusion

We have considered the volatility smile phenomenon generated by two-asset European style options under a continuous-time two-state Markov chain regime-switching model. Because of the difficulty to find closed-form solution of the Feynman–Kac style formula, an algorithm for a numerical solution was designed. We confirmed the suitability of the OS scheme by conducting convergence test and comparing with ADI scheme. While the volatility smile is observed to obviate the constant-volatility assumption of the Black–Scholes model, the regime-switching model has the clear advantage that it implies the volatility smile structure through the model itself. In addition, the regime-switching model has relatively simple additional parameters $(\lambda, \sigma_x(i), \sigma_y(i), \rho_{xy})$ to realize an appropriate volatility smile compared to the Black–Scholes model. One needs to estimate the parameters λ, $\sigma_x(i)$, $\sigma_y(i)$, and ρ_{xy} to apply the model in practice. The estimation procedure is given in Zhang (2001).

Acknowledgments

The first author (J.S. Kim) was supported by the National Institute for Mathematical Sciences (NIMS) grant funded by the Korea government (No. A21301). The corresponding author (D.H. Shin) was supported by Inha University and a Korea University Grant.

References

Buffington, J., & Elliott, R. J. (2002). American options with regime switching. *International Journal of Theoretical and Applied Finance*, *5*(5), 497–514.

Chin, R. C. Y., Manteuffel, T. A., & Pillis, J. de (1984). ADI as a preconditioning for solving the convection–diffusion equation. *SIAM Journal on Scientific Computing*, *5*(2), 281–299.

Duffy, D. J. (2006). *Finite difference methods in financial engineering: a partial differential equation approach*. New York: John Wiley and Sons.

Fouque, J. P., Papanicolaou, G., & Sircar, K. R. (2000). *Derivatives in financial markets with stochastic volatility*. Cambridge University Press.

Hamilton, J. D. (1989). A new approach to the economic analysis of non-stationary time series. *Econometrica*, *57*, 357–384.

Haug, E. G. (1997). *The complete guide to option pricing formulas*. New York: McGraw-Hill.

Hout, K. J., & Foulon, S. (2010). ADI finite difference schemes for option pricing in the Heston model with correlation. *International Journal of Numerical Analysis and Modeling*, *7*(2), 303–320.

Hull, J. C. (2000). *Options, futures, and other derivatives* (4th ed.). New Jersy: Prentice-Hall.

Ikonen, S., & Toivanen, J. (2004). Operator splitting methods for American option pricing. *Applied Mathematics Letters*, *17*, 809–814.

Jeong, D., & Kim, J. (2013). A comparison study of ADI and operator splitting methods on option pricing models. *Journal of Computational and Applied Mathematics*, *247*, 162–171.

Kim, M. A., Jang, B.-G., & Lee, H.-S. (2008). A first-passage-time model under regime-switching market environment. *Journal of Banking and Finance*, *32*, 2617–2627.

Yao, D. D., Zhang, Q., & Zhou, X. Y. (2006). A regime-switching model for European options. Stochastic processes, optimization, and control theory applications in financial engineering, queueing networks, and manufacturing systems. In H. M. Yan, G. Yin, & Q. Zhnag (Eds.), *International series in operations research and management sciences* (pp. 281–300). New York: Springer-SBM.

Yin, G., & Zhang, Q. (1998). *Continuous-time Markov chains and applications*. New York: Springer.

Yin, G., & Zhou, X. Y. (2003). Markowits's mean–variance portfolio selection with regime-switching: from discrete-time models to their continuous-time limits. *IEEE Transactions on Automatic Control*, *43*(3), 349–360.

Zhang, Q. (2001). Stock trading: an optimal selling rule. *SIAM Journal on Control and Optimization*, *40*(1), 64–87.

Junseok Kim received his Ph.D. in Applied Mathematics from the University of Minnesota, U.S.A. in 2002. He also received his B.S. degree from the Department of Mathematics Education, Korea University, Korea in 1995. He joined the faculty of Korea University, Korea in 2008 where he is currently an associate professor at the Department of Mathematics. His research interests are in computational finance and computational fluid dynamics.

Darae Jeong received her Ph.D. in Applied Mathematics from Korea University, Korea, in 2013. And she received M.S. degree in Applied Mathematics and B.S. degree in Mathematics from Korea University in 2011 and Dongguk University in 2008, respectively. She is currently working as a post-doctoral research fellow at the Department of Mathematics, Korea University, Korea. Her research interests include computational finance, computational fluid dynamics, and scientific computation.

Dong-Hoon Shin received his Ph.D. in Mathematics from the University of Georgia in 2009. He also received his M.S. and B.S. degrees from the Department of Mathematics of Korea University at Seoul and Chungnam, Republic of Korea in 2003 and 2000 respectively. Currently he is an Assistant Professor with the Division of Global Finance and Banking at the Inha University at Incheon, Republic of Korea. His research interests include optimal control, regime-switching, derivatives pricing, and applications of derivatives for finance.